Neural circuits for somatosensory control of auditory thalamocortical processing

Michael Lohse*[1], Johannes C. Dahmen[1], Victoria M. Bajo[1], Andrew J. King[1]

[1]Department of Physiology, Anatomy, and Genetics. University of Oxford, Oxford OX1 3PT, United Kingdom.

*Correspondence should be addressed to M.L. (michael.lohse@dpag.ox.ac.uk) or A.J.K. (andrew.king@dpag.ox.ac.uk)

ACKNOWLEDGMENTS

The research was funded by a Wellcome Trust Studentship (WT105241/Z/14/Z) to M.L., and a Wellcome Trust Principal Research Fellowship (WT108369/Z/2015/Z) to A.J.K.

AUTHOR CONTRIBUTIONS

M.L. conceived and designed the research. M.L. performed research and analyzed the data. M.L. and J.C.D. performed surgeries. M.L. and A.J.K. acquired funding for the research. A.J.K. provided infrastructure and resources. A.J.K, J.C.D., and V.B.L. supervised the research. M.L., J.C.D., V.B.L. and A.J.K. interpreted the research. M.L., J.C.D., V.B.L. and A.J.K wrote the manuscript.

CONFLICT OF INTEREST

The authors declare no conflict of interest

Abstract

To form a coherent representation of the environment, the brain must integrate information across different senses. Such multisensory convergence is widespread at the level of the cortex, where it is thought to arise primarily from corticocortical connections. Much less is known about the role of subcortical circuits in shaping the multisensory properties of cortical neurons. We show that sound-evoked activity in the mouse auditory cortex is widely suppressed by whisker stimulation. This suppression depends on the primary somatosensory cortex (S1), but surprisingly is implemented through a circuit linking S1 and the auditory thalamocortical system via the auditory midbrain. We also show that an additional, direct pathway exists from S1 to the medial sector of auditory thalamus, which facilitates auditory responses in neurons that do not project to the auditory cortex. The thalamus thus occupies a pivotal role in integrating multisensory signals by somatosensory top-down control of auditory subcortical processing.

Introduction

Having multiple sensory systems, each specialized for the transduction of a different type of physical stimulus, maximizes our ability to gather information about the external world and helps us cope when one stimulus type is not available. In the dark, for instance, we can still hear and touch our environment even though we may not be able to see anything. Furthermore, when the same event or object is registered by more than one sense, as is often the case, our chances of detecting and accurately evaluating its biological significance dramatically increase[1]. This requires that information provided by different sensory systems is combined in the brain.

Apart from specialized subcortical nuclei, such as the superior colliculus, it is widely assumed that multisensory processing is most prevalent at the level of the cerebral cortex[1,2]. Evidence for multisensory convergence has been found in nearly all cortical areas, including the primary sensory cortices. In the primary auditory cortex (A1), for example, visual or tactile stimuli can modulate acoustically-driven activity, most commonly by suppressing responses to sound[3–6]. Unlike audition and vision, the sense of touch informs an organism exclusively about objects in its immediate vicinity. Such nearby objects may require urgent and dedicated processing. A mechanism that gives precedence to somatosensory information over cues from other modalities may therefore be advantageous to the organism's survival. The suppression of sound-evoked activity in auditory cortical neurons by the somatosensory system is likely the result of such a mechanism.

The circuitry underlying crossmodal influences on processing in early sensory cortical areas is poorly understood. Because visual, auditory and somatosensory cortices innervate each other and receive inputs from higher-level, association areas[3,5,7–12], most studies have focused on the role of intracortical circuits in multisensory integration[13–16]. This, however, ignores the potential contribution of ascending inputs from the thalamus, which may also provide a source of multisensory input to primary cortical areas, such as A1[9,17–20], or the possibility that early sensory cortical areas may communicate via trans-thalamic pathways[21,22].

We show that somatosensory inputs exert a powerful influence on processing in the auditory system, which takes the form of divisive suppression in the auditory cortex. Dissecting the underlying circuitry, we found that this suppression originates in the primary somatosensory cortex (S1) and is implemented via S1-recipient neurons in the auditory midbrain, which inhibit sound-driven activity in the auditory thalamocortical system. We also show that a parallel crossmodal corticothalamic pathway from S1 to the medial sector of the auditory thalamus allows for somatosensory drive and facilitation of auditory responses in thalamic neurons that do not project to the auditory cortex. These

results demonstrate that the auditory thalamus has an essential role in integrating somatosensory and auditory inputs and in shaping the multisensory properties of cortical and other downstream neurons.

Results

Somatosensory influences on primary auditory cortex

Because variable effects of tactile stimulation have been reported on the activity of neurons in the auditory cortex of different species[4,5,23–25], we recorded extracellular activity in A1, identified by its tonotopic gradient, while presenting sounds to mice and simultaneously deflecting their whiskers (**Fig. 1a**). We consistently found that concurrent whisker stimulation reduced auditory responses evoked by both tones (**Fig. 1b-d**) and noise bursts (**Fig. 1e,f**), demonstrating widespread suppression of auditory activity in A1. Assessment of the input-output responses across all tones presented, normalized to the firing rate at each neuron's best frequency (BF), revealed that this suppression was of a divisive nature, with strong effects around the BF and negligible effects for off-BF responses that were closer to baseline activity (**Fig. 1d**).

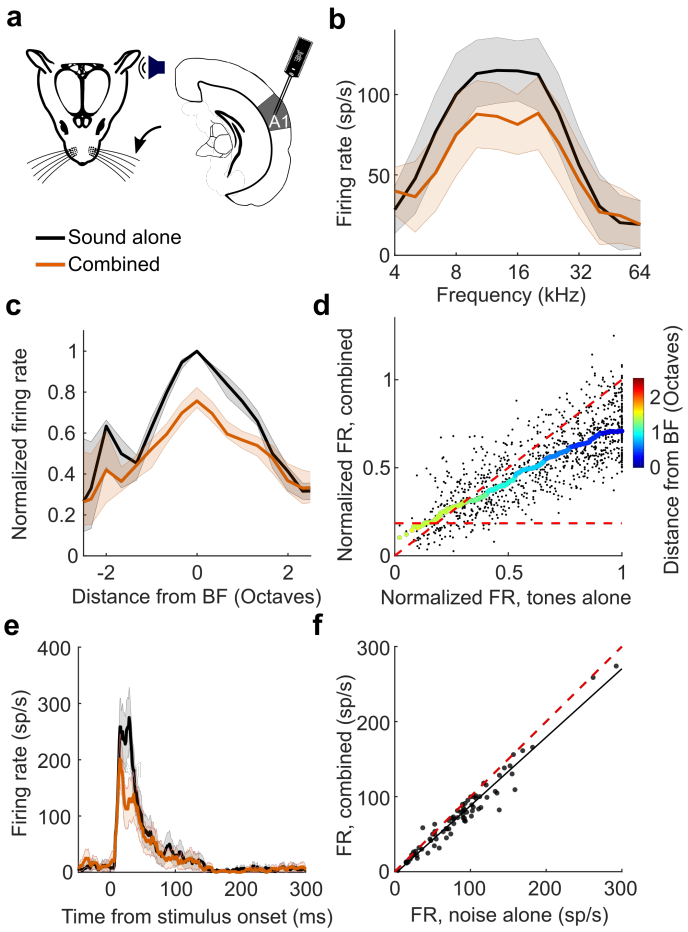

59 **Figure 1. Somatosensory suppression of neurons in primary auditory cortex.**

60 **a)** Schematic of recording setup. **b)** Frequency tuning curves with (orange) and without (black) whisker deflection
61 from an example unit in A1. **c)** Median frequency tuning across all tuned A1 units with and without whisker
62 deflection (change in BF response: $P < 0.001$, $n = 77$, 4 mice). **d)** Relationship between normalized firing rate (FR)
63 to tones across all frequencies and all units (black dots) with ('combined') or without ('tones alone') whisker
64 stimulation. Thick multi-colored line denotes the running median of this relationship (window: 0.1 normalized
65 firing rate), and the colors denote distance from BF. The horizontal dashed red line denotes the median
66 normalized spontaneous rate across units. The diagonal dashed red line is the line of equality. A larger distance
67 between the multi-colored line and the diagonal line at the blue end than at the red end indicates divisive scaling.
68 **e)** An A1 example unit's responses to broadband noise with (orange) and without (black) concurrent whisker
69 stimulation. **f)** Summary of A1 units' responses to noise alone vs noise with whisker deflection ($P < 0.001$, $n =$
70 81, 4 mice). FR, firing rate. The red dashed line indicates the line of equality. The black solid line indicates the
71 least squares linear fit. Shaded area indicates 95% confidence intervals of the mean (**b,e**) or 95% nonparametric
72 confidence intervals of the median (**c**).

73 **Somatosensory influences on auditory thalamus**

74 To investigate the circuitry underlying this extensive modulation of auditory cortical processing, we
75 first set out to determine whether the activity of subcortical auditory neurons is similarly affected by
76 whisker stimulation. We found no evidence for somatosensory-auditory interactions in the central
77 nucleus of the inferior colliculus (CNIC) (**Supplementary Fig. 1**) and therefore focused on the medial
78 geniculate body (MGB), the main thalamic gateway to the auditory cortex. We recorded from neurons
79 in the lateral region of the MGB, including both the lemniscal ventral division (MGBv) and the non-
80 lemniscal dorsal division (MGBd) (**Fig. 2, Supplementary Fig. 2**). Whisker stimulation suppressed
81 responses to noise and to tones near the BF of neurons in both MGBv and MGBd (**Fig. 2b-d;**
82 **Supplementary Fig. 3**). As in the cortex, this suppression took the form of a divisive scaling of the
83 sound-evoked response (**Fig. 2e,f**). Whisker stimulation alone did not affect the activity of neurons in
84 either MGBv or MGBd (**Supplementary Fig. 3**).

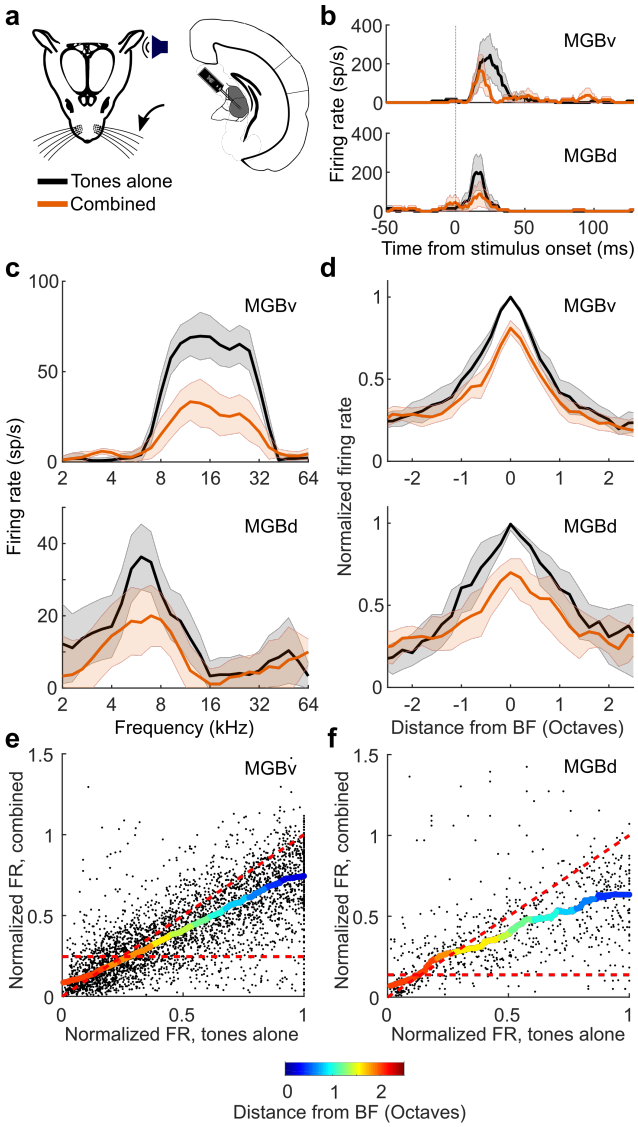

Figure 2. Divisive scaling of frequency tuning in the MGBv and MGBd

a) Schematic of recording setup. **b)** Examples of PSTHs illustrating BF responses with (orange) or without (black) concurrent whisker stimulation from units in MGBv and MGBd. **c)** Examples of frequency tuning curves with or without concurrent whisker stimulation from units in MGBv and MGBd. **d)** Median tuning curve across units recorded in MGBv (change in BF response: $P < 0.001$, $n = 145$) or MGBd (change in BF response, $P < 0.001$, $n = 31$) with or without concurrent whisker stimulation. Shaded area indicates the 95% confidence intervals of the means (**b,c**), or the 95% nonparametric confidence intervals of the median (**d**). **e,f)** Relationship between normalized firing rate (FR) for all units (black dots) recorded in the MGBv (**e**) and MGBd (**f**) in response to tones across all frequencies presented either with ('combined') or without ('tones alone') whisker stimulation. Thick multi-colored lines show the running median of this relationship (window: 0.1 normalized firing rate), and the colors denote distance from BF. The horizontal dashed red line denotes the median normalized spontaneous rate across units. The diagonal dashed red line is the line of equality. A larger distance between the multi-colored line and the diagonal line at the blue end than at the red end indicates divisive scaling. $n_{MGBv} = 145$ (9 mice); $n_{MGBd} = 31$ (9 mice).

The medial section of the auditory thalamus contains several divisions, medial MGB (MGBm), the posterior intralaminar nucleus (PIN), and the suprageniculate nucleus (SGN), which are anatomically distinct from the MGBv and MGBd[26–28]. In the MGBm/PIN and SGN, we found units that were directly driven by whisker inputs alone (**Fig 3a,c,i**). We also found that the responses of individual units to noise (**Fig 3a,b,d,i**) or tones (**Fig 3i**) could be either facilitated or suppressed when combined with whisker input. Units in which responses to tones were facilitated exhibited an increase in firing rate across the entire frequency tuning curve, indicative of additive scaling (**Fig. 3e,f**), whereas suppressed units, similar to those in MGBv/d and cortex, showed divisive scaling (**Fig. 3g,h**). Thus, neurons in the medial section of the auditory thalamus were influenced by whisker stimulation in a much more heterogeneous fashion than neurons in the lateral MGB (**Fig 3j**).

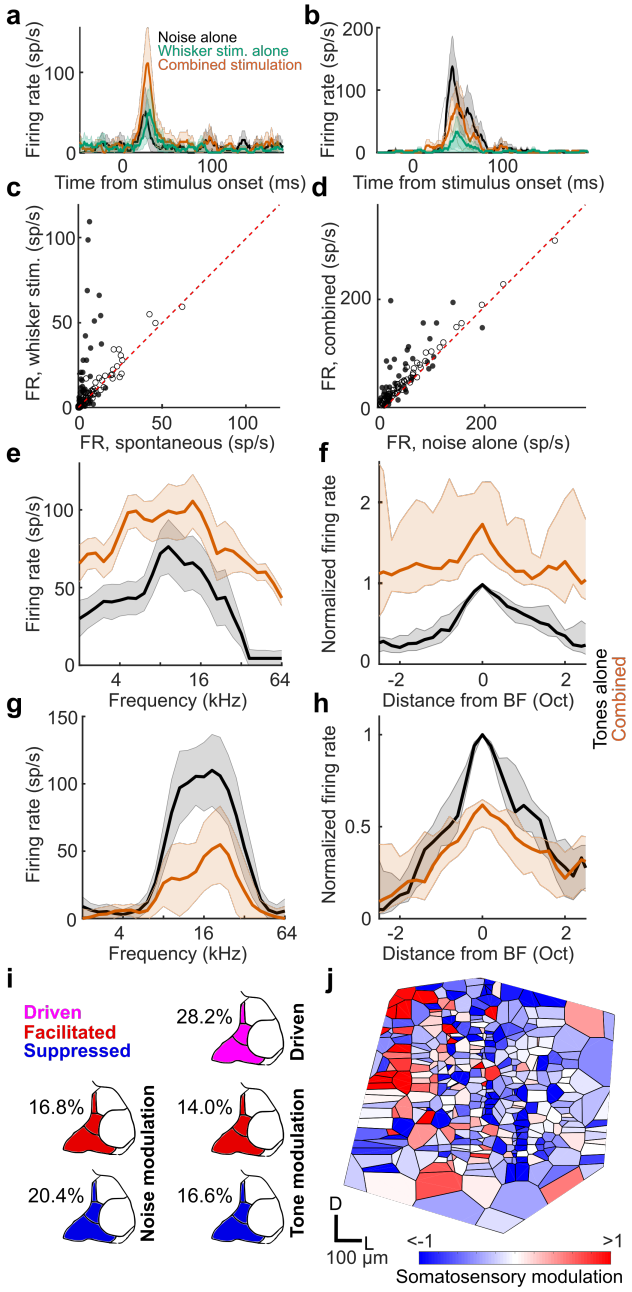

Figure 3. Diverse somatosensory influences on neurons in MGBm/PIN and SGN

a,b) Example PSTHs of responses to broadband noise recorded in MGBm/PIN/SGN with (orange) and without (black) concurrent whisker stimulation, as well as whisker stimulation alone (green) showing facilitation (**a**, $P < 0.05$, paired *t*-test) and suppression (**b**, $P < 0.05$, paired *t*-test) of the auditory response, respectively. **c)** Summary of responses (firing rate, FR) to whisker stimulation alone vs spontaneous activity in the medial sector of the auditory thalamus. Filled circles indicate units driven by somatosensory stimulation ($P < 0.05$, *t*-test). **d**) Summary of responses to broadband noise combined with or without concurrent whisker stimulation. Filled circles indicate significantly ($P < 0.05$, paired *t*-test) modulated units (n = 113, 8 mice). **e**) Example frequency tuning curves for tones with (orange) and without (black) concurrent whisker stimulation for a unit showing crossmodal facilitation ($P < 0.05$, paired *t*-test). **f)** Summary tuning curves of units with significantly facilitated BF responses. **g,h)** Same as **e-f** for units with significantly suppressed BF responses. $n_{facilitated} = 32$, $n_{suppressed} = 27$, 12 mice. Shaded area indicates 95% confidence intervals of the mean (**a,b,e,g**) or nonparametric confidence intervals of the medians (**f,h**), respectively. **i)** Percentage of neurons in the MGBm/PIN and SGN significantly ($P < 0.05$, one-sided *t*-test) driven by somatosensory input, or showing significant modulation ($P < 0.05$, two sided *t*-test) of the responses to noise or tones at BF when combined with somatosensory input. **j)** Voronoi diagram illustrating somatosensory modulation in all tuned neurons across auditory thalamus. Each patch represents the location of one extracellularly recorded thalamic unit (n = 369, 14 mice) and is color-coded for the type and strength of somatosensory modulation (red, facilitation; blue, suppression).

Somatosensory inhibition of auditory cortex is inherited from the thalamus

Whisker-stimulation induced suppression of auditory activity is therefore present subcortically, particularly in the MGBv and MGBd, two auditory thalamic subdivisions with massive thalamocortical projections. This suggests that cortical neurons may inherit signals in which acoustic and somatosensory information have already been integrated. To investigate whether MGB neurons do indeed relay a whisker-modulated signal to auditory cortex, we expressed the calcium indicator GCaMP6m in the entire auditory thalamus and measured calcium transients in thalamocortical boutons in layer 1 of the auditory cortex[28] (**Fig. 4a,b**). Layer 1 of the mouse auditory cortex tends to receive more diverse thalamic inputs than layers 3b/4. In A1, for example, layer 1 combines dense projections from MGBv[28,29] with projections from other structures, such as MGBm[28] and the lateral posterior nucleus of the thalamus[19]. Nevertheless, whisker stimulation had a suppressive effect on responses to both noise (**Fig. 4c,d**) and tones (**Fig. 4e,f**). Similar to neurons in MGBv, MGBd and auditory cortex, frequency-tuned thalamocortical boutons exhibited divisive scaling with the largest response reduction at BF (**Fig. 4e,f**). We did not find any auditory thalamocortical boutons that were driven by whisker stimulation alone or whose sound responses were facilitated by whisker stimulation. This suggests that only somatosensory suppression of auditory activity is projected to the auditory cortex, whereas the facilitation observed in the medial sector of the auditory thalamus is not.

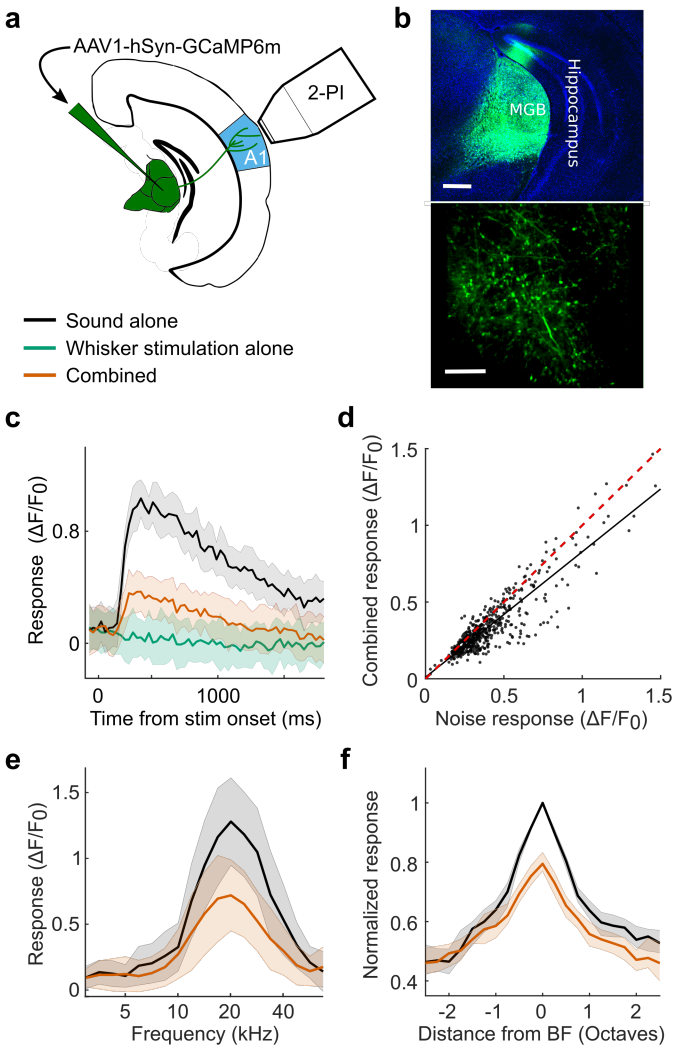

Figure 4: Thalamic inputs to auditory cortex are suppressed by whisker stimulation

a) Schematic of recording setup. **b)** *Top:* Confocal image of GCaMP6m expression in the auditory thalamus. Scale bar, 400 µm. *Bottom: In vivo* 2-photon image of thalamocortical boutons in layer 1 of the auditory cortex. Scale bar, 20 µm. **c)** Calcium response of an example thalamic bouton in layer 1 responding to broadband noise with (orange) or without (black) concurrent whisker deflection, as well as to whisker deflection alone (green). **d)** Summary of responses to noise alone vs combined noise plus whisker deflection in all noise-responsive thalamocortical boutons ($P < 0.001$, $n = 512$, 3 mice). The red dashed line indicates the line of equality. The black solid line indicates the least squares linear fit. **e)** Frequency tuning curves with (orange) and without (black) whisker deflection from an example thalamocortical bouton. **f)** Median frequency tuning curves across all frequency tuned boutons (change in BF response: $P < 0.001$, $n = 310$, 3 mice). Shaded area indicates the 95% confidence intervals of the means (**c,e**), or the 95% nonparametric confidence intervals of the median (**f**).

S1 mediates suppression of the auditory thalamus

To determine whether the primary somatosensory cortex (S1) is involved in whisker-stimulation induced suppression of the auditory thalamocortical system, we recorded neuronal activity in the

MGB of VGAT-ChR2-YFP mice whilst silencing S1 optogenetically (**Fig. 5a** and **Supplementary Fig. 4**). Silencing S1 did not affect spontaneous activity or tone-evoked auditory thalamic responses (**Supplementary Fig. 5**), but significantly reduced the capacity of whisker stimulation to suppress the BF responses of neurons in both MGBv and MGBd (**Fig. 5b,c**; see **Supplementary Fig. 6** for further corroboration using the opsin Jaws for S1 silencing). Thus, S1 is a critical part of the circuitry mediating the somatosensory control of auditory thalamocortical responses.

Silencing S1 also had a similar effect on the responses of neurons in the medial sector of the auditory thalamus that were otherwise robustly suppressed by whisker stimulation (**Supplementary Fig. 7**), but did not affect the capacity of whisker stimulation to enhance responses in this part of the thalamus (**Supplementary Fig. 7**). S1 is thus necessary for somatosensory suppression throughout the auditory thalamus, but not for somatosensory facilitation. That S1 activation is also sufficient for the suppression of auditory thalamocortical responses was revealed when we optogenetically activated infragranular cells in S1 via the red-shifted opsin ChrimsonR and measured calcium transients in thalamocortical boutons (**Fig. 5d,e**). Optogenetic S1 activation suppressed their responses to noise bursts (**Fig. 5f,g**) and thus replicated the previously observed whisker-induced suppression of auditory thalamocortical boutons.

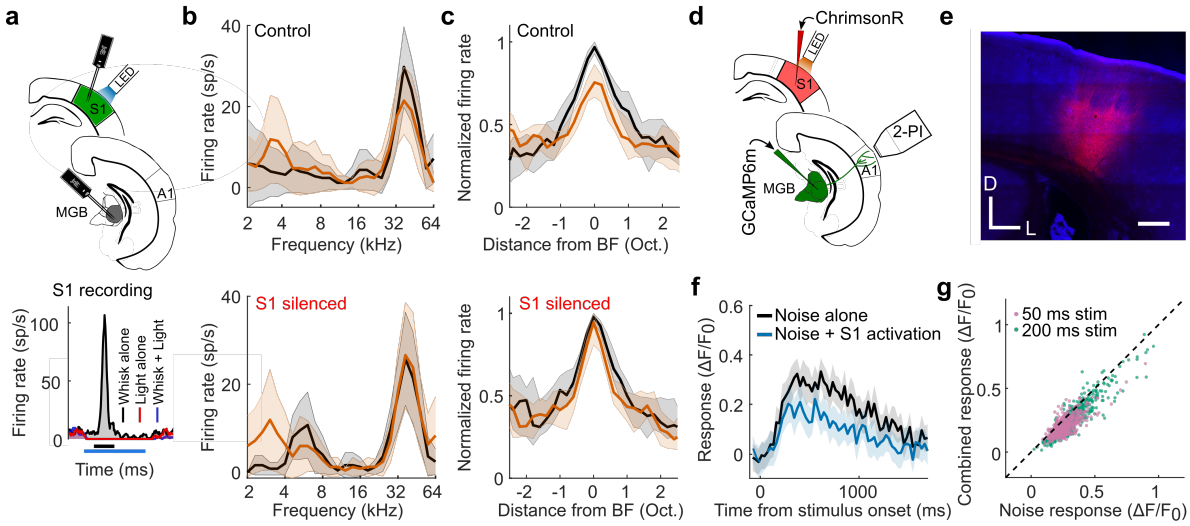

Figure 5: S1 mediates somatosensory suppression of auditory thalamocortical axons

a) *Top:* Schematic of optogenetic targeting of somatosensory cortex in VGAT-ChR2 mice and electrophysiological recording setup. *Bottom:* Example PSTHs of a unit recorded in S1, demonstrating the effect of optogenetic suppression of somatosensory cortex on spontaneous activity and whisker-stimulation evoked responses. Bars below the x-axis indicate timing of whisker stimulation (black) and light stimulation for silencing S1 (blue). **b)** Frequency tuning curves of an example MGBv unit based on tone responses with (orange) and without (black) concurrent whisker stimulation during the control condition (top) and when S1 was silenced (bottom). **c)** Median tuning curves of all units recorded in MGBv/d with (orange) and without whisker deflection (black) during the

control condition (top) and when S1 was silenced (bottom). The suppressive effect of whisker stimulation on the BF response of MGBv/d neurons was reduced following S1 silencing (P = 0.014, n = 59, 3 mice). **d)** Schematic of experimental setup for combined 2-photon thalamocortical bouton imaging with optogenetic activation of S1. **e)** Confocal image showing expression of ChrimsonR-tdTomato in infragranular layers of S1. Scale bar, 300 µm. **f)** Calcium response of an example thalamic bouton in layer 1 of the auditory cortex, illustrating suppression of the response to a 50 ms noise burst by optogenetic S1 stimulation. Shading indicates 95% confidence intervals around the mean. The 3rd and 4th imaging frames of the S1 stimulation condition displayed a large light artefact from the LED and have therefore been removed. **g)** Summary plot of responses to noise alone or noise combined with infragranular S1 stimulation for all noise-responsive boutons. Purple and green points indicate responses to 50 ms and 200 ms noise stimulation, respectively. n_{50ms} = 539, 8 imaging fields, 1 mouse; n_{200ms} = 652, 7 imaging fields, 2 mice. Shaded area indicates the 95% confidence intervals of the means (**b,f**), or the 95% nonparametric confidence intervals of the median (**c**).

Auditory cortex does not mediate somatosensory influences on auditory thalamus

One way in which S1 could suppress neuronal activity in the auditory thalamus is via an indirect corticocorticothalamic route that takes advantage of the massive corticothalamic projections originating in the auditory cortex. However, while silencing auditory cortex strongly decreased both spontaneous activity (**Supplementary Fig. 5**) and sound-evoked responses in MGBv and MGBd neurons (**Supplementary Fig. 5**), we observed no change in either the response suppression evoked in these neurons by whisker stimulation (**Supplementary Fig. 8**) or in the response facilitation exhibited by neurons located in the medial sector of the auditory thalamus (**Supplementary Fig. 8**).

S1 projection neurons account for auditory thalamic facilitation

To investigate whether a direct corticothalamic projection[22,30,31] exists that could mediate somatosensory control over auditory thalamus, we performed viral tracing experiments in S1 corticothalamic neurons. These revealed that a projection does indeed exist, which originates from RBP4-expressing layer 5 neurons in S1 and densely innervates the medial sector of auditory thalamus (**Fig. 6a-c**), particularly the PIN (**Fig. 6b,c**). Optical stimulation of these S1 layer 5 neurons significantly altered the spontaneous firing rate of more than a third of recorded units (**Fig. 6d,e**), suggesting a direct excitatory pathway from S1 to the medial auditory thalamus. Activation of this pathway also replicated the additive scaling of the frequency response profiles of auditory neurons recorded in this region of the auditory thalamus (**Fig. 6f,g**) that we observed when combining sounds and whisker stimulation.

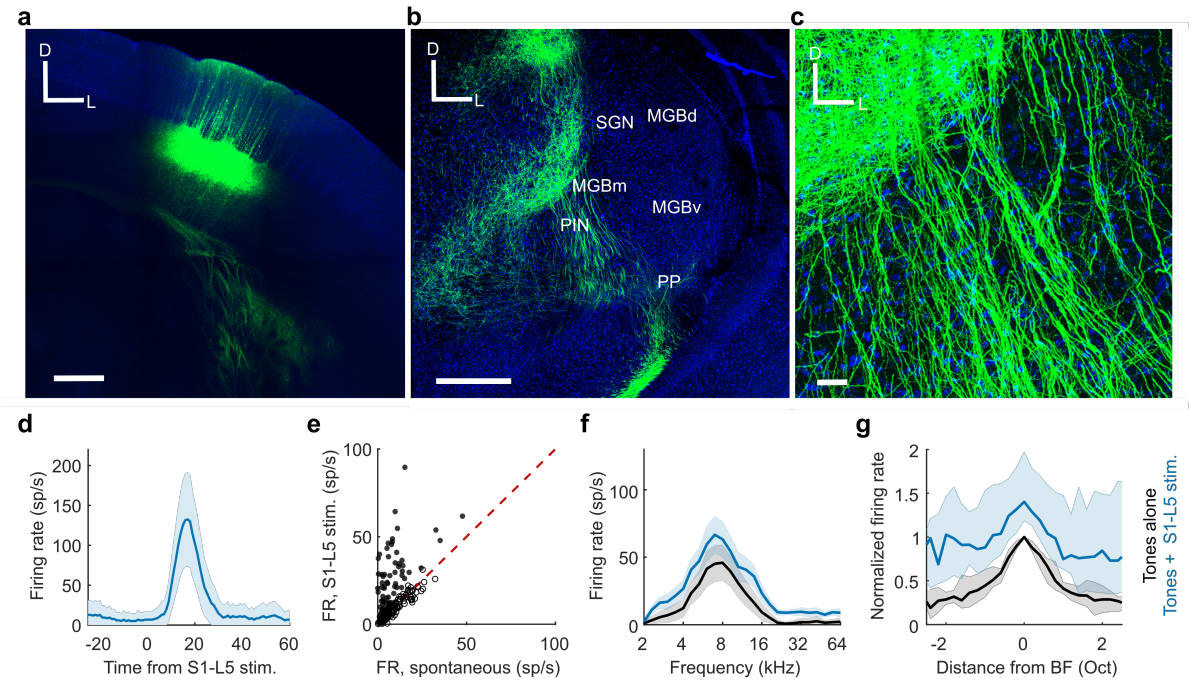

Figure 6: Direct pathway from S1 to MGBm/PIN and SGN

a) Confocal image of ChR2-YFP expression in RBP4+ cells in layer 5 (L5) of S1. Scale bar, 400 µm; D, dorsal; L, lateral. **b)** Confocal image of a coronal section of the thalamus showing S1-L5 (RBP4+) axons in the medial sector of the auditory thalamus. PP, peripeduncular nucleus. Scale bar, 400 µm. **c)** High magnification image showing S1-L5 (RBP4+) axons in MGBm/PIN. Blue = DAPI, Green = YFP. Scale bar, 30 µm. **d)** Example unit located in MGBm/PIN that was driven by stimulation of S1-L5 (RBP4+) neurons. **e)** Summary of MGBm/PIN neuronal firing rate (FR) responses to 50 ms light pulses delivered to stimulate S1-L5 (RBP4+) neurons. n = 183, 5 mice. Filled circles indicate the 69 units in which spontaneous firing was significantly altered ($p < 0.05$, t-test) by S1-L5 stimulation. **f)** Tuning curves from an example unit in MGBm/PIN in which the auditory response was significantly enhanced by concurrent stimulation of S1-L5 (RBP4+) neurons. **g)** Median tuning curves from units in the medial sector of auditory thalamus with significantly ($p < 0.05$, paired t-test) facilitated BF responses during stimulation of S1-L5 (RBP4+) neurons. n = 25, 5 mice. Shaded areas indicate 95% confidence intervals of the means (**d,f**) or 95% nonparametric confidence intervals of the medians (**g**), respectively. BF responses were significantly modulated in 18% (13.7% facilitated, 4.4% suppressed; n= 183, 5 mice) of units in MGBm/PIN and SGN by concurrent stimulation of S1-L5 (RBP4+) neurons.

Although these findings are consistent with a facilitatory influence of layer 5 projection neurons in S1 on neurons in the medial auditory thalamus, selective stimulation of the RBP4-expressing neurons did not induce suppression of the sound-evoked responses of neurons recorded in the MGBv and MGBd (**Supplementary Fig. 9**). This result can be readily accounted for given the generally excitatory nature of corticofugal projections and the predominantly medial termination pattern of this particular pathway, as well as the relative paucity of GABAergic interneurons in the rodent MGB[32]. Nevertheless, the lack of effect from stimulation of S1 RBP4-expressing neurons on the

sound-evoked responses of neurons recorded in the lateral auditory thalamus contrasts with the reduced influence of whisker stimulation on those responses when S1 was silenced optogenetically. This therefore implies the existence of another pathway by which S1 neurons can influence auditory processing in this part of the thalamus.

A corticocollicular pathway for somatosensory thalamic suppression

The final objective was to identify the source of inhibition mediating S1-dependent suppression of neuronal activity in the auditory thalamus. One major source of inhibitory input to the MGB, and a structure that has previously been implicated in crossmodal thalamic processing[33], is the thalamic reticular nucleus (TRN). By optogenetically silencing the auditory sector of TRN (AudTRN) during tone presentation, we found that this part of the thalamus can modulate the excitability of MGB neurons (**Fig. 7a-c**). Surprisingly, however, we did not find any evidence that AudTRN neurons play a role in mediating somatosensory suppression of the MGB (**Fig. 7d,e**).

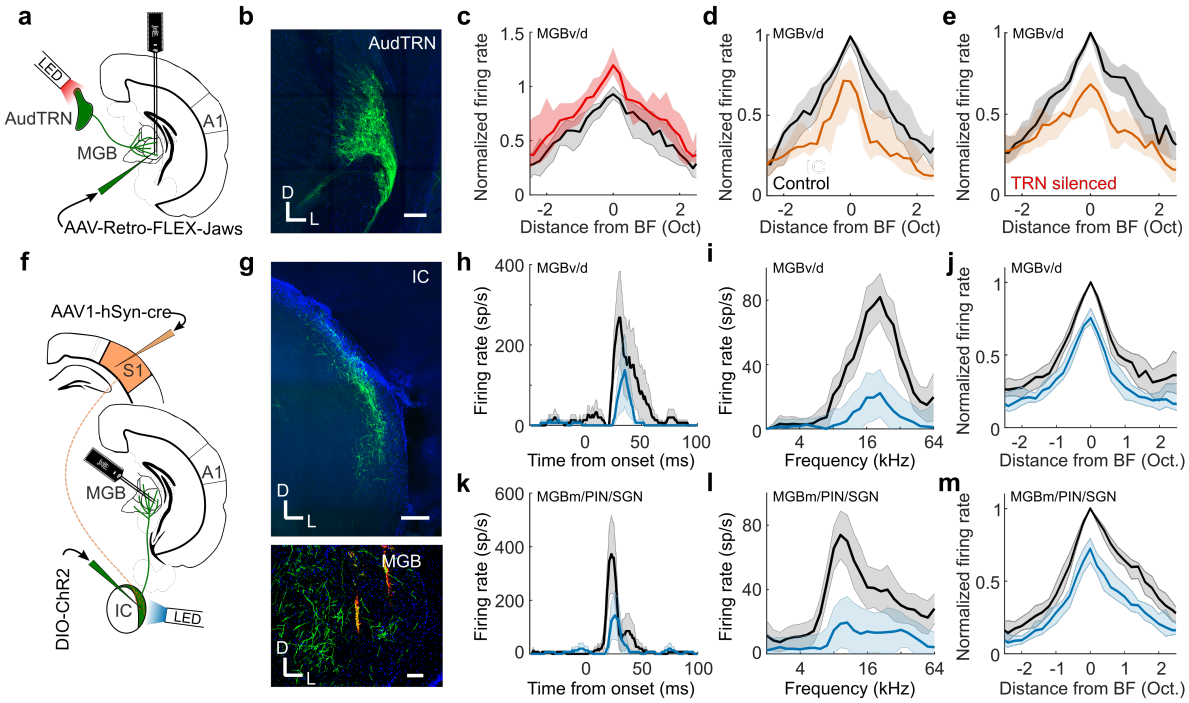

Figure 7: Corticocollicular circuit mediates somatosensory suppression of the thalamus

a) Schematic of experimental paradigm in **b-e. b)** GABAergic cells in TRN retrogradely-labelled with Jaws from auditory thalamus. Scale bar, 150 µm. **c)** Summary (median) frequency tuning curve across MGBv/d units with (red) or without (black) optogenetic suppression of AudTRN activity (change in BF firing response, $P < 0.001$, n = 38, 2 mice). **d-e)** Median frequency tuning curve of MGBv/MGBd units illustrating suppression induced by concurrent whisker stimulation (orange) with AudTRN either unaffected (**d**) or optogenetically suppressed (**e**). Silencing AudTRN had no effect on the whisker-induced suppression of auditory responses in MGBv/MGBd (P = 0.83, n = 38, 2 mice). **f)** Schematic of experimental paradigm in **g-m**. **g)** *Top:* ChR2-YFP expression in neurons in the shell of IC, labelled by anterograde transport of cre from S1 (AAV1-hSyn-cre) and a cre-dependent AAV5-

263 DIO-ChR2-eYFP injected into the IC. Scale bar, 200 µm. *Bottom:* Axons (green) of anterogradely labelled IC
264 neurons in MGB. Scale bar, 100 µm. Orange marks show DiI tracts from the recording probe in the MGB. D,
265 dorsal; L, lateral. **h)** Example PSTHs illustrating BF responses of an MGBv unit with (blue) and without (black)
266 optogenetic stimulation of S1-recipient IC neurons. **i)** Example frequency tuning curve of an MGBv unit with
267 (blue) and without (black) optogenetic stimulation of S1-recipient IC neurons. **j)** Median MGBv/MGBd tuning
268 curve with (blue) and without (black) stimulation of S1-recipient IC neurons: -20.9% median change in BF firing
269 rate ($P < 0.001$; $n = 85$, 3 mice). **k-m**) same as **h-j** for units recorded in MGBm/PIN/SGN. **m**) -26.9% median
270 change in BF firing rate ($P < 0.001$; $n = 89$, 3 mice). Shaded area illustrates the 95% confidence intervals of the
271 means (**h,i,k,l**), or the 95% nonparametric confidence intervals of the median (**c,d,e,j,m**).

272 Inhibitory input to the MGB can also arrive from extra-thalamic sources, including the IC[34–36],
273 which provides its major source of ascending input. Interestingly, descending inputs from the
274 somatosensory cortex appear to target modular zones containing GABAergic neurons within the
275 lateral shell of the mouse IC[34], suggesting a possible route by which whisker stimulation could
276 influence auditory processing. In order to selectively target IC neurons that receive input from S1, we
277 employed an anterograde transsynaptic viral tagging approach[37], which involved injecting AAV1-hSyn-
278 cre into S1. Combining this with an injection into the IC of a virus that cre-dependently expresses both
279 channelrhodopsin-2 and eYFP, we were able to show that S1 targets a subset of IC shell neurons (**Fig**
280 **7f,g**) and that these neurons project to the auditory thalamus (**Fig 7g**). Furthermore, activating these
281 S1-recipient IC neurons induced suppression of auditory responses both in MGBv/d (**Fig. 7h-j**) and the
282 medial auditory thalamus (**Fig. 7k-m**). This demonstrates that S1 exerts suppressive control over
283 auditory thalamic processing via a corticocolliculothalamic pathway, in addition to its facilitatory
284 influence via a direct crossmodal corticothalamic pathway (**Fig. 8**).

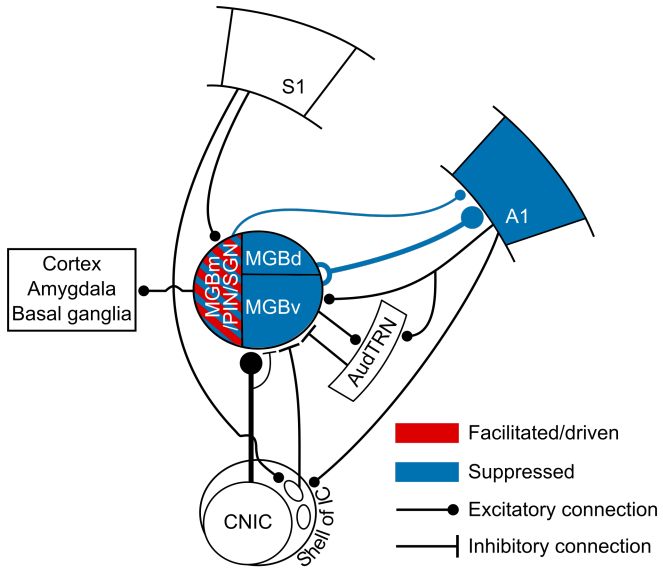

Figure 8: Circuits enabling somatosensory control of the auditory thalamocortical system.

Auditory responses in the regions of the auditory thalamus and cortex depicted in blue were suppressed by concurrent whisker stimulation via a descending pathway from S1 to the lateral shell of IC, which then projects to the MGB. Some neurons in the medial sector of the auditory thalamus were driven or had their auditory responses enhanced by whisker stimulation (depicted in red), which can be mediated by a direct corticothalamic projection from S1 to MGBm/PIN/SGN.

Discussion

Our results demonstrate that the somatosensory system exerts a powerful influence over sound processing in both the auditory cortex and thalamus. These effects are diverse and anatomically specific. We identified two separate corticofugal pathways (**Fig. 8**), which both originate in S1 but exert opposing somatosensory control over the auditory thalamus. First, a crossmodal descending pathway via the auditory midbrain mediates somatosensory divisive suppression in the auditory thalamocortical system. Second, a direct corticothalamic pathway targets the medial sector of auditory thalamus, through which S1 drives spiking activity and facilitates neuronal responses that are not transmitted to the auditory cortex.

Multisensory integration in the auditory cortex

Multisensory interactions occur throughout the cerebral cortex, however, including early sensory areas[1,2]. Although spiking responses to visual or somatosensory stimuli have been found in different parts of auditory cortex, the commonest type of crossmodal interaction is seen when otherwise ineffective stimuli are paired with a sound[3–6,16,23,24,38,39]. Diverse modulatory effects on auditory cortical

306 processing have been reported in these studies, and, in line with our results, several have found that
307 crossmodal suppressive interactions are particularly prevalent, both in rodents[4,19,25] and other
308 species[3,5,6,40].

309 **Auditory cortex inherits multisensory signals from the thalamus**

310 The search for the source of these non-auditory influences on auditory cortical activity has focused
311 principally on other cortical areas. Direct connections between early sensory cortical areas have been
312 widely reported in different species[3,5,7–11]. Furthermore, in mice, optogenetic stimulation of A1
313 corticocortical projections can modulate the activity[13,14] and stimulus selectivity[14] of neurons in
314 primary visual cortex via local inhibitory circuits. These studies therefore highlight the importance of
315 intracortical connections in mediating multisensory interactions.

316 Non-auditory influences on auditory cortical processing can also be inherited from the
317 thalamus. Anatomical studies have emphasized the potential contribution to multisensory processing
318 in the auditory cortex of extralemniscal thalamic input, not just from non-primary regions of the MGB,
319 such as the MGBm, but also from areas like the SGN and the pulvinar[9,41,42]. Indeed, in mice, the
320 suppressive effects of visual looming stimuli on A1 activity appear to be mediated by the lateral
321 posterior nucleus, the rodent homologue of the primate pulvinar[19]. However, A1 receives the great
322 majority of its ascending input from the MGBv, which is traditionally viewed as a unisensory structure.
323 Nevertheless, cutaneous electrical stimulation has been shown to modulate auditory responses in the
324 MGBv[17,20], and our findings demonstrate that the sound-evoked responses of most neurons recorded
325 there and in the MGBd are suppressed by concurrent whisker stimulation. Moreover, we observed
326 comparable crossmodal suppression in auditory thalamocortical axon boutons and in A1 neurons,
327 strongly suggesting that somatosensory-auditory interactions are inherited by these cortical neurons
328 from their primary source of thalamic input.

329 **Multisensory processing in the auditory thalamus**

330 In the MGBv and MGBd, the strongest suppressive effects induced by whisker stimulation occurred at
331 the BF of the neurons, i.e. the tone frequency at which the largest response was obtained. This
332 crossmodal divisive scaling by non-driving sensory inputs resembles that found in primate cortex[43–45].
333 The divisive normalization operating in these areas is thought to be a canonical feature of multisensory
334 integration, which can account for the way neuronal responses depend on the efficacy and spatial
335 relationship of the individual stimuli[44]. Our results suggest that this may be a more widespread
336 property of multisensory neurons, even occurring in a structure (i.e. the auditory thalamus) that lacks
337 recurrent connectivity[46].

338 In contrast to the exclusively suppressive effects of somatosensory stimulation on the activity
339 of neurons in the MGBv and MGBd, neurons in the medial sector of the auditory thalamus (MGBm,
340 PIN and SGN) exhibited a mixture of crossmodal suppression and enhancement and >25% were driven
341 by whisker stimulation. Somatosensory responses have previously been reported in these areas in
342 other species[47,48]. Neurons in these medial structures primarily target secondary auditory and higher-
343 level association cortical areas, and the minority that innervate A1 terminate in layer 1 and layer
344 5/6[28,49,50]. However, the thalamic axon boutons that we imaged in layer 1 showed exclusively
345 crossmodal suppression of sound-evoked activity, suggesting that neurons whose responses are
346 facilitated or driven by somatosensory inputs project elsewhere in the brain.

347 Neurons in the medial auditory thalamus also innervate subcortical areas implicated in
348 decision making and emotional processing, including the basal ganglia[28,51] and amygdala[28,48,49,52]. In
349 particular, the projection to the amygdala is a critical part of the circuitry mediating auditory fear
350 conditioning[52–54]. In addition to differences in their efferent targets, neurons in the MGBm, PIN and
351 SGN have distinct physiological properties from those in the MGBv/MGBd[55]. Furthermore, the lack of
352 excitatory connectivity between these neurons[46] makes the auditory thalamus an ideal place to
353 establish functionally distinct pathways that are independently and flexibly modulated by contextual
354 information, including inputs from other senses or motor commands[22].

355 **Corticofugal crossmodal control of the auditory thalamus**

356 There is growing evidence that descending corticofugal pathways contribute to the processing of
357 sensory information, both within and across sensory modalities, and to integrating sensory and motor
358 signals[22,30,31,56,57]. We found that activity in S1 can modulate sound-evoked responses throughout the
359 auditory thalamus, and therefore in the auditory cortex, demonstrating the existence of a
360 transthalamic pathway for mediating the influence of somatosensory stimuli on auditory cortical
361 processing. Furthermore, S1 is an essential component of the circuitry underlying the suppressive
362 effects of whisker stimulation on auditory function. Although auditory cortical feedback can inhibit
363 MGB activity via GABAergic neurons in the TRN[58], this pathway does not appear to be involved in the
364 somatosensory suppression of auditory responses. Instead, this depends on a descending projection
365 from S1 to IC shell neurons that inhibit responses in the MGB. Somatosensory dominance over
366 auditory processing in mouse A1 is therefore implemented by a corticocolliculo-thalamocortical
367 circuit.

368 Interactions between somatosensory and auditory inputs occur as early as the cochlear
369 nucleus in the brainstem[59]. We did not observe any effects of whisker stimulation on the auditory
370 responses of neurons recorded in the CNIC, the primary relay nucleus of the auditory midbrain,

371 suggesting that multisensory suppression in the MGBv is unlikely to be inherited from earlier in the
372 auditory pathway. However, the lateral shell of the IC receives somatosensory inputs from much of
373 the body via projections from the somatosensory cortex and the brainstem[34,60]. In mice, these inputs
374 target GAD-67-positive modules that are separated by regions receiving auditory inputs[34].
375 Furthermore, GABAergic neurons throughout the IC project to the MGB[35,36,61,62]. Our data therefore
376 bridge these anatomical studies and establish a functional role for such circuits by demonstrating that
377 a relatively small population of S1-recipient neurons in the lateral shell of the IC are responsible for
378 the suppressive effects of whisker stimulation on sound-evoked responses in the auditory thalamus.

379 Although optogenetic activation of S1 layer 5 neurons drove activity and had a facilitatory
380 effect on the auditory responses of neurons in the medial sector of auditory thalamus, silencing S1 did
381 not eliminate the crossmodal facilitation induced by whisker stimulation. However, somatosensory
382 inputs also reach this part of the thalamus via spinothalamic, dorsal column and trigeminal
383 pathways[63–65], providing additional and potentially redundant routes by which somatosensory signals
384 can influence processing in the medial auditory thalamus.

385 **Perceptual implications of somatosensory control over auditory processing**

386 Given its key position in the sensory and motor systems of the brain, context-dependent modulation
387 of neuronal activity in the thalamus has wide-ranging consequences for information processing, not
388 only in the cerebral cortex but also in other thalamorecipient brain regions, such as the amygdala and
389 basal ganglia. The presence of region-specific multisensory interactions throughout the auditory
390 thalamus therefore implies that combining information from different sensory modalities at this
391 relatively early stage in the processing hierarchy plays a fundamental role in how animals perceive and
392 interact with their sensory environments.

393 In rats, facial touch is associated with inhibition of the auditory cortex[4], potentially reflecting
394 a greater salience of haptic information during social interactions and exploration. Our data suggest
395 that these effects are likely to be present in the thalamus too and that they are asymmetric since we
396 did not observe a comparable modulatory influence of the sounds used in this study on neuronal
397 responses to whisker stimulation in the somatosensory thalamus or cortex (**Supplementary Fig. 10**).
398 The suppressive effects of somatosensory stimulation on sound-evoked responses, which have now
399 been reported at multiple stages of the auditory pathway, may also help to reduce the impact of
400 vocalizations or other self-generated and potentially distracting sounds, such as those resulting from
401 chewing or breathing[59].

402 A reduction in the firing rate of auditory neurons in the presence of other sensory cues can be
403 accompanied by an increase in response reliability and in the amount of stimulus-related information
404 transmitted[3,66]. Furthermore, auditory cortical activity is suppressed when an animal engages in a
405 task[67]. Of particular relevance to the present study is the finding that divisive scaling of auditory
406 cortical frequency tuning is associated with improved frequency discrimination at the expense of
407 impaired tone detection[57]. By inducing divisive gain in the auditory thalamocortical system,
408 somatosensory inputs might function as a bottom up cue that sharpens auditory acuity, whilst
409 reducing sensitivity.

410 Data availability

411 All relevant data are available on request to, and will be fulfilled by, the lead contact
412 (michael.lohse@dpag.ox.ac.uk).

413 Code availability

414 Matlab code for analyses are available on request to, and will be fulfilled by, the lead
415 contact (michael.lohse@dpag.ox.ac.uk).

416 References

417 1. Murray, M. M. & Wallace, M. T. *The neural bases of multisensory processes*. (CRC Press/Taylor
418 & Francis, 2012).

419 2. Choi, I., Lee, J. Y. & Lee, S. H. Bottom-up and top-down modulation of multisensory integration.
420 *Curr. Opin. Neurobiol.* **52**, 115–122 (2018).

421 3. Bizley, J. K., Nodal, F. R., Bajo, V. M., Nelken, I. & King, A. J. Physiological and anatomical
422 evidence for multisensory interactions in auditory cortex. *Cereb. Cortex* **17**, 2172–2189 (2007).

423 4. Rao, R. P., Mielke, F., Bobrov, E. & Brecht, M. Vocalization-whisking coordination and
424 multisensory integration of social signals in rat auditory cortex. *Elife* **3**, 1–20 (2014).

425 5. Meredith, M. A. & Allman, B. L. Single-unit analysis of somatosensory processing in the core
426 auditory cortex of hearing ferrets. *Eur. J. Neurosci.* **41**, 686–698 (2015).

427 6. Kayser, C., Petkov, C. I. & Logothetis, N. K. Visual modulation of neurons in auditory cortex.
428 *Cereb. Cortex* **18**, 1560–1574 (2008).

429 7. Rockland, K. S. & Ojima, H. Multisensory convergence in calcarine visual areas in macaque
430 monkey. *Int. J. Psychophysiol.* **50**, 19–26 (2003).

431 8. Cappe, C. & Barone, P. Heteromodal connections supporting multisensory integration at low
432 levels of cortical processing in the monkey. *Eur. J. Neurosci.* **22**, 2886–2902 (2005).

433 9. Budinger, E., Heil, P., Hess, A. & Scheich, H. Multisensory processing via early cortical stages:
434 Connections of the primary auditory cortical field with other sensory systems. *Neuroscience*
435 **143**, 1065–1083 (2006).

436 10. Banks, M. I., Uhlrich, D. J., Smith, P. H., Krause, B. M. & Manning, K. A. Descending projections
437 from extrastriate visual cortex modulate responses of cells in primary auditory cortex. *Cereb.*
438 *Cortex* **21**, 2620–2638 (2011).

439 11. Stehberg, J., Stehberg, J., Dang, P. T. & Frostig, R. D. Unimodal primary sensory cortices are
440 directly connected by long-range horizontal projections in the rat sensory cortex. *Front.*
441 *Neuroanat.* **8**, 1–19 (2014).

442 12. Zingg, B. *et al.* Neural networks of the mouse neocortex. *Cell* **156**, 1096–1111 (2014).

443 13. Iurilli, G. *et al.* Sound-driven synaptic inhibition in primary visual cortex. *Neuron* **73**, 814–828
444 (2012).

445 14. Ibrahim, L. A. *et al.* Cross-modality sharpening of visual cortical processing through layer-1-
446 mediated inhibition and disinhibition. *Neuron* **89**, 1031–1045 (2016).

447 15. Song, Y.-H. *et al.* A neural circuit for auditory dominance over visual perception. *Neuron* **93**,
448 940–954 (2017).

449 16. Atilgan, H. *et al.* Integration of visual information in auditory cortex promotes auditory scene
450 analysis through multisensory binding. *Neuron* **97**, 640–655 (2018).

451 17. Kimura, A. & Imbe, H. Robust subthreshold cross-modal modulation of auditory response by
452 cutaneous electrical stimulation in first- and higher-order auditory thalamic nuclei.
453 *Neuroscience* **372**, 161–180 (2018).

454 18. Wu, C., Stefanescu, R. A., Martel, D. T. & Shore, S. E. Listening to another sense: somatosensory
455 integration in the auditory system. *Cell Tissue Res.* **361**, 233–250 (2015).

456 19. Chou, X. L. *et al.* Contextual and cross-modality modulation of auditory cortical processing
457 through pulvinar mediated suppression. *Elife* **9**, 1–21 (2020).

458 20. Khorevin, V. I. Effect of electrodermal stimulation on single unit responses to acoustic
459 stimulation in the parvocellular part of the medial geniculate body. *Neurophysiology* **12**, 129–
460 134 (1980).

461 21. Sherman, S. M. & Guillery, R. W. Distinct functions for direct and transthalamic corticocortical
462 connections. *J. Neurophysiol.* **106**, 1068–1077 (2011).

463 22. Lohse, M., Bajo, V. M. & King, A. J. Development, organization and plasticity of auditory circuits:
464 Lessons from a cherished colleague. *Eur. J. Neurosci.* **49**, 990–1004 (2019).

465 23. Fu, K. G. *et al.* Auditory cortical neurons respond to somatosensory stimulation. *J. Neurosci.* **23**,
466 7510–7515 (2003).

467 24. Kayser, C., Petkov, C. I., Augath, M. & Logothetis, N. K. Integration of touch and sound in
468 auditory cortex. *Neuron* **48**, 373–384 (2005).

469 25. Zhang, M., Kwon, S. E., Ben-Johny, M., O'Connor, D. H. & Issa, J. B. Spectral hallmark of
470 auditory-tactile interactions in the mouse somatosensory cortex. *Commun. Biol.* **3**, 1–17
471 (2020).

472 26. Lu, E., Llano, D. A. & Sherman, S. M. Different distributions of calbindin and calretinin
473 immunostaining across the medial and dorsal divisions of the mouse medial geniculate body.
474 *Hear. Res.* **257**, 16–23 (2009).

475 27. Anderson, L. A. & Linden, J. F. Physiological differences between histologically defined
476 subdivisions in the mouse auditory thalamus. *Hear. Res.* **274**, 48–60 (2011).

477 28. Vasquez-Lopez, S. A. *et al.* Thalamic input to auditory cortex is locally heterogeneous but
478 globally tonotopic. *Elife* **6**, 1:18 (2017).

479 29. Takesian, A. E., Bogart, L. J., Lichtman, J. W. & Hensch, T. K. Inhibitory circuit gating of auditory
480 critical-period plasticity. *Nat. Neurosci.* **21**, 218–227 (2018).

481 30. Allen, A. E., Procyk, C. A., Brown, T. M. & Lucas, R. J. Convergence of visual and whisker
482 responses in the primary somatosensory thalamus (ventral posterior medial region) of the
483 mouse. *J. Physiol.* **595**, 865–881 (2017).

484 31. Mo, C. & Sherman, S. M. A sensorimotor pathway via higher-order thalamus. *J. Neurosci.*
485 (2018).

486 32. Winer, J. A. & Larue, D. T. Evolution of GABAergic circuitry in the mammalian medial geniculate

487 body. *Proc Natl Acad Sci U S A* **93**, 3083–3087 (1996).

488 33. Kimura, A., Yokoi, I., Imbe, H., Donishi, T. & Kaneoke, Y. Auditory thalamic reticular nucleus of
489 the rat: Anatomical nodes for modulation of auditory and cross-modal sensory processing in
490 the loop connectivity between the cortex and thalamus. *J. Comp. Neurol.* **520**, 1457–1480
491 (2012).

492 34. Lesicko, A. M. H., Hristova, T. S., Maigler, K. C. & Llano, D. A. Connectional modularity of top-
493 down and bottom-up multimodal inputs to the lateral cortex of the mouse inferior colliculus.
494 *J. Neurosci.* **36**, 11037–11050 (2016).

495 35. Clarke, B. A. & Lee, C. C. Inhibitory projections in the mouse auditory tectothalamic system.
496 *Brain Sci.* **8**, (2018).

497 36. Beebe, N. L., Mellott, J. G. & Schofield, B. R. Inhibitory projections from the inferior colliculus
498 to the medial geniculate body originate from four subtypes of GABAergic Cells. *eNeuro* **5**, 1–13
499 (2018).

500 37. Zingg, B. *et al.* AAV-mediated anterograde transsynaptic tagging: Mapping corticocollicular
501 input-defined neural pathways for defense behaviors. *Neuron* **93**, 33–47 (2017).

502 38. Ghazanfar, A. A., Maier, J. X., Hoffman, K. L. & Logothetis, N. K. Multisensory integration of
503 dynamic faces and voices in rhesus monkey auditory cortex. *J. Neurosci.* **25**, 5004–5012 (2005).

504 39. Lakatos, P., Chen, C., Connell, M. N. O., Mills, A. & Schroeder, C. E. Neuronal oscillations and
505 multisensory interaction in primary auditory cortex. *Neuron* **53**, 279–292 (2007).

506 40. Perrodin, C., Kayser, C., Logothetis, N. K. & Petkov, C. I. Natural asynchronies in audiovisual
507 communication signals regulate neuronal multisensory interactions in voice-sensitive cortex.
508 *Proc. Natl. Acad. Sci. U. S. A.* **112**, 273–278 (2015).

509 41. De La Mothe, L. A., Blumell, S., Kajikawa, Y. & Hackett, T. A. Thalamic connections of the
510 auditory cortex in marmoset monkeys: Core and medial belt regions. *J. Comp. Neurol.* **496**, 72–
511 96 (2006).

512 42. Smiley, J. F. & Falchier, A. Multisensory connections of monkey auditory cerebral cortex. *Hear.*
513 *Res.* **258**, 37–46 (2009).

514 43. Avillac, M., Ben Hamed, S. & Duhamel, J.-R. Multisensory integration in the ventral intraparietal
515 area of the macaque monkey. *J. Neurosci.* **27**, 1922–1932 (2007).

516 44. Ohshiro, T., Angelaki, D. E. & Deangelis, G. C. A normalization model of multisensory
517 integration. *Nat. Neurosci.* **14**, 775–782 (2011).

518 45. Ohshiro, T., Angelaki, D. E. & DeAngelis, G. C. A neural signature of divisive normalization at the
519 Level of multisensory integration in primate cortex. *Neuron* **95**, 399–411 (2017).

520 46. Bartlett, E. L. & Smith, P. H. Anatomic, intrinsic, and synaptic properties of dorsal and ventral
521 division neurons in rat medial geniculate body. *J. Neurophysiol.* **81**, 1999–2016 (1999).

522 47. Wepsic, J. G. Multimodal sensory activation of cells in the magnocellular medial geniculate
523 nucleus. *Exp. Neurol.* **15**, 299–318 (1966).

524 48. Bordi, F. & LeDoux, J. E. Response properties of single units in areas of rat auditory thalamus
525 that project to the amygdala - I. Acoustic discharge patterns and frequency receptive fields.
526 *Exp. Brain Res.* **98**, 261–274 (1994).

527 49. Doron, N. N. & Ledoux, J. E. Cells in the posterior thalamus project to both amygdala and
528 temporal cortex: A quantitative retrograde double-labeling study in the rat. *J. Comp. Neurol.*
529 **425**, 257–274 (2000).

530 50. Huang, C. L. & Winer, J. A. Auditory thalamocortical projections in the cat: Laminar and areal
531 patterns of input. *J. Comp. Neurol.* **427**, 302–331 (2000).

532 51. Moriizumi, T. & Hattori, T. Ultrastructural morphology of projections from the medial
533 geniculate nucleus and its adjacent region to the basal ganglia. *Brain Res. Bull.* **29**, 193–198
534 (1992).

535 52. Barsy, B. *et al.* Associative and plastic thalamic signaling to the lateral amygdala controls fear
536 behavior. *Nat. Neurosci.* 1–13 (2020). doi:10.1038/s41593-020-0620-z

537 53. Cruikshank, S. J., Edeline, J. M. & Weinberger, N. M. Stimulation at a site of auditory-
538 somatosensory convergence in the medial geniculate nucleus is an effective unconditioned
539 stimulus for fear conditioning. *Behav Neurosci* **106**, 471–483 (1992).

540 54. Weinberger, N. M. The medial geniculate, not the amygdala, as the root of auditory fear
541 conditioning. *Hear. Res.* **274**, 61–74 (2011).

542 55. Smith, P. H., Bartlett, E. L. & Kowalkowski, A. Unique combination of anatomy and physiology
543 in cells of the rat paralaminar thalamic nuclei adjacent to the medial geniculate body. *J. Comp.*
544 *Neurol.* **496**, 314–334 (2006).

545 56. Bajo, V. M. & King, A. J. Cortical modulation of auditory processing in the midbrain. *Front.*
546 *Neural Circuits* **6**, 1–12 (2013).

547 57. Guo, W., Clause, A. R., Barth-Maron, A. & Polley, D. B. A corticothalamic circuit for dynamic
548 switching between feature detection and discrimination. *Neuron* **95**, 180–194 (2017).

549 58. Zhang, Z. *et al.* Corticofugal projection inhibits the auditory thalamus through the thalamic
550 reticular nucleus. *J. Neurophysiol.* **99**, 2938–2945 (2008).

551 59. Shore, S. E. & Zhou, J. Somatosensory influence on the cochlear nucleus and beyond. *Hear. Res.*
552 **216**–**217**, 90–99 (2006).

553 60. Aitkin, L. M., Kenyon, C. E. & Philpott, P. The representation of the auditory and somatosensory
554 systems in the external nucleus of the cat inferior colliculus. *J. Comp. Neurol.* **196**, 25–40
555 (1981).

556 61. Peruzzi, D., Bartlett, E., Smith, P. H. & Oliver, D. L. A monosynaptic GABAergic input from the
557 inferior colliculus to the medial geniculate body in rat. *J. Neurosci.* **17**, 3766–77 (1997).

558 62. Winer, J. A., Mariet, R. L. Saint, Larue, D. T. & Oliver, D. L. GABAergic feedforward projections
559 from the inferior colliculus to the medial geniculate body. **93**, 8005–8010 (1996).

560 63. Jones, E. G. & Burton, H. Cytoarchitecture and somatic sensory connectivity of thalamic nuclei
561 other than the ventrobasal complex in the cat. *J. Comp. Neurol.* **154**, 395–432 (1974).

562 64. Lund, R. D. & Webster, K. E. Thalamic afferents from the spinal cord and the trigeminal nucleus.
563 An experiment anatomic study in the rat. *J. Comp. Neurol.* **130**, 313–328 (1967).

564 65. Lund, R. D. & Webster, K. E. Thalamic afferents from the dorsal column nuclei. An experimental
565 anatomical study in the rat. *J. Comp. Neurol.* **130**, 301–311 (1967).

566 66. Kayser, C., Logothetis, N. K. & Panzeri, S. Visual enhancement of the information
567 representation in auditory cortex. *Curr. Biol.* **20**, 19–24 (2010).

568 67. Otazu, G. H., Tai, L. H., Yang, Y. & Zador, A. M. Engaging in an auditory task suppresses
569 responses in auditory cortex. *Nat. Neurosci.* **12**, 646–654 (2009).

Methods

Mice

All experiments were approved by the Committee on Animal Care and Ethical Review at the University of Oxford and were licensed by the UK Home Office (Animal Scientific Procedures Act, 1986, amended in 2012). Four strains of male and female mice were used: *C57BL6/J* (Envigo, UK), *VGAT-ChR2-YFP* (JAX 014548 - Jackson Laboratories, USA), *VGAT-cre* (JAX 016962 - Jackson Laboratories, USA), and *C57BL6/NTac.Cdh23*. *C57BL6/J*. *C57BL6/J, VGAT-ChR2-YFP*, and *VGAT-cre* mice were 7–12 weeks old, and *C57BL6/NTac.Cdh23* mice[68] were 10–20 weeks old at the time of data collection. All experiments were carried out in a sound-attenuated chamber.

Stimuli

Auditory stimuli were programmed and controlled in custom-written Matlab code (https://github.com/beniamino38/benware) and generated via TDT RX6 (electrophysiology) or RZ6 (2-photon imaging) microprocessors. Sounds were generated at a ~200 kHz sampling rate, amplified by a TDT SA1 stereo amplifier and delivered via a modified (i.e. sound was 'funnelled' into an otoscope speculum) Avisoft ultrasonic electrostatic loudspeaker (Vifa - electrophysiology) or a TDT EC1 electrostatic speaker (imaging) positioned ~1 mm from the entrance to the ear canal. The sound presentation system was calibrated to a flat (±1 dB) frequency-level response between 1 and 64 kHz. Stimuli included pure tones, covering a frequency range from 2 to 64 kHz, and broadband noise bursts (1-64 kHz). All sounds included 5-ms linear amplitude onset/offset ramps, and unless specified otherwise were presented at 80 dB SPL.

Whisker deflections were delivered with a piezoelectric bimorph attached to a small glass tube. During stimulation, most whiskers were positioned inside the stimulation tube and deflected in a single cosine wave (valley-to-valley), transiently displacing the whiskers 1 mm from resting position at a speed of 40 mm/s.

Presentation of acoustic and whisker stimuli was randomly interleaved, with each sensory stimulus having a duration of 50 ms, unless otherwise specified.

Extracellular recordings

We carried out extracellular recordings using 32- or 64-channel silicon probes (NeuroNexus Technologies Inc.) in a 4 × 8, 8 × 8 or 2 × 32 electrode configuration. Prior to insertion, probes were coated with DiI (Sigma-Aldrich) for subsequent histological verification of the recording sites. Data were acquired using a RZ2 BioAmp processor (TDT) and custom-written Matlab code

601 (https://github.com/beniamino38/benware). Mice were anesthetized with an intraperitoneal
602 injection of ketamine (100 mg kg^{-1}) and medetomidine (0.14 mg kg^{-1}). Intraperitoneal injections of
603 atropine (Atrocare, 1 mg kg^{-1}) to prevent bradycardia and reduce bronchial secretions and
604 dexamethasone (Dexadreson, 4 mg kg−1) to prevent brain edema were administered. Prior to the
605 surgery, the analgesic bupivacaine was injected under the scalp. The depth of anesthesia was
606 monitored via the pedal reflex and adjusted via small additional doses of the ketamine/medetomidine
607 mix (1/5th of the initial dose) given subcutaneously approximately every 15 min once the recordings
608 had started (~1–1.5 h post induction of anesthesia).

609 All recordings were performed in the right hemisphere. A silver reference wire was positioned
610 in the visual cortex of the contralateral hemisphere, and a grounding wire was attached under the skin
611 on the neck musculature. The head was fixed in position with a metal bar attached with bone cement
612 to the skull over the left hemisphere. Circular craniotomies (2 mm diameter) were performed above
613 the IC (centered ~5 mm posterior from bregma and ~1 mm lateral from midline), over the visual
614 cortex for auditory thalamic recordings (centered ~3 mm caudal from bregma and ~2.1 mm lateral
615 from midline), and/or over A1 (centered ~2.5 mm posterior from bregma and ~4.5 mm lateral from
616 midline). The exposed dura mater was kept moist with saline throughout the experiment.

617 Recording sites were considered to be in the CNIC when the units recorded on those sites
618 were part of a clear dorso-ventral tonotopic gradient[69,70] and the probe's location could be confirmed
619 by post-mortem brain histology. For recordings in the MGB, probe sites were attributed to specific
620 auditory thalamic subdivisions by histological reconstruction of the recording sites (**Supplementary**
621 **Fig. 2**). We parcellated the auditory thalamus based on previous immunohistochemical descriptions[26]
622 and our own pilot tracing experiments from several cortical areas. Accordingly, recording sites were
623 assigned to the ventral division (MGBv), dorsal division (MGBd), medial division and posterior
624 intralaminar nucleus (MGBm/PIN), or suprageniculate nucleus (SGN). Based on these histological
625 reconstructions, recording sites attributed to the MGBv were located <500 µm from the lateral border
626 of the MGB and <500 µm from the deepest acoustically-responsive site, while those in the MGBd were
627 <500 µm from the lateral border of the MGB, but >500 µm from the most ventral acoustically-
628 responsive site. For recordings in the medial sector of the auditory thalamus, sites assigned to the
629 MGBm/PIN were >500 µm from the lateral border of the MGB and <500 µm from the most ventral
630 acoustically-responsive site, and those in the SGN were >500 µm from the lateral border of the MGB
631 and >500 µm from the most ventral acoustically-responsive site.

632 A1 was identified by robust neuronal responses to broadband noise bursts, and a well-defined
633 caudo-rostral tonotopic axis[28,71]. Cortical tonotopy was assessed in all cortical recordings by estimating

634 frequency response areas from responses to pure tones using probes with four recording shanks
635 spaced 200 µm apart and oriented parallel to the caudo-rostral axis.

636 Two-photon calcium imaging of thalamocortical boutons

637 We made injections of ~140 nl (diluted 1:1 in PBS) of AAV1.Syn.GCaMP6m.WPRE.SV40 into the
638 auditory thalamus (3 mm caudal from bregma, 2.1 mm lateral from midline and 2.8 - 3 mm ventral
639 from the cortical surface) for expression of GCaMP6m in auditory thalamic neurons and axons as
640 reported previously[28]. Mice were administered buprenorphine (Vetergesic 1 ml/kg), dexamethasone
641 (Dexadreson 4 µg), and atropine (Atrocare 1 µg) intraperitoneally and anesthetized with 1.5%
642 isoflurane throughout the surgical procedure. An additional dose of buprenorphine was given 24 hours
643 post-operatively.

644 In order to visualize the calcium activity of thalamic boutons in layer 1 (20-80 µm below the
645 surface) of the auditory cortex, mice were chronically implanted with a head bar and a circular 4 mm
646 diameter glass window. The implant surgery procedure took place 2-3 weeks following injection of the
647 viral construct. Data acquisition began ~7 days after the implant surgery. Calcium imaging was carried
648 out using a 2-photon laser scanning microscope (B-Scope, Thorlabs, USA). Excitation light of 930 nm
649 (10-50 mW power measured under the objective) was provided by a Mai-Tai eHP (Spectra-Physics,
650 USA) laser fitted with a DeepSee prechirp unit (70 fs pulse width, 80 MHz repetition rate). The laser
651 beam was directed through a Conoptics (CT, USA) modulator and scanned onto the brain with an 8
652 kHz resonant scanner (x-axis) and a galvanometric scan mirror (y-axis), allowing acquisition of 512x512
653 pixel frames at ~30 Hz. Emitted photons were guided through a 525/50 filter onto GaAsP
654 photomultipliers (Hamamatsu, Japan). We used ScanImage[72] to control the microscope during data
655 acquisition and a 16X immersion objective (Nikon, Japan). Mice were kept anesthetized with a mixture
656 of ketamine and medetomidine throughout the experiment (similar to the experiments described in
657 the previous section).

658 Viral injections and transgenic expression of proteins for optogenetic control

659 All injections were performed using a custom-made pressure injection system with a calibrated glass
660 pipette positioned in the right hemisphere. The tip of the pipette was carefully and slowly inserted
661 into the area of interest, and ~20 nl boluses were then given every two minutes until the desired
662 volume had been injected. The pipette was then left in position for an additional 5 minutes before
663 being slowly retracted. All optogenetic experiments involving viral injections were carried out >3
664 weeks after the injection to allow for expression of the opsin.

665 *Activating infragranular cells in S1 using ChrimsonR whilst imaging auditory thalamocortical*
666 *axons and boutons*
667 We injected 120 nL of AAV1-CAG-ChrimsonR[73] in S1 (-0.8 and -1.0 mm caudal from bregma, 2.6 mm
668 lateral from midline, and 0.8, 0.65, and 0.5 mm ventral from the cortical surface) to induce expression
669 in the infragranular layers of S1 of C57BL6/J mice. In the same surgery, we also injected AAV1-hSyn-
670 GCaMP6m into auditory thalamus and implanted a glass window over the auditory cortex and a head
671 bar, as explained in the previous section. Finally, in the same surgery, we placed a 400 µm fibre optic
672 cannula on the dura of S1. For optogenetic activation, a 5-7 mW/mm^2, 595 nm LED pulse (Doric Lenses,
673 Canada) was delivered to S1 concurrently with, and for the duration of, broadband noise stimulation
674 (i.e. 50 ms or 200 ms).

675 *Activating RBP4+ cells in layer 5 of S1 using ChR2*
676 We injected 60-80 nl of AAV5-DIO-hChR2-eYFP[74] in S1 (0.8 mm caudal from bregma, 2.6 mm lateral
677 from midline, and 1.0 mm, and 0.95 and 0.9 mm ventral from the cortical surface) of RBP4-cre mice
678 to induce expression of ChR2 in layer 5 neurons. For optogenetic activation, a 5-7 mW/mm^2, 465 nm
679 LED pulse (Doric Lenses) was presented. Light was delivered through a 1 mm fibre acutely positioned
680 on the dura mater above S1 and concurrently with, and for the duration of, sound stimulation (i.e. 50
681 ms).

682 *Suppressing neuronal activity in the auditory sector of thalamic reticular nucleus using Jaws*
683 In order to transfect cells in the auditory sector of TRN (audTRN) with Jaws, we exploited the fact that
684 the MGB in rodents contains very few inhibitory cells[32]. An injection of 140 nL of the cre-dependent
685 retrograde construct pAAV-CAG-FLEX-rc[Jaws-KGC-GFP-ER2][75,76] into the MGB (3.0 mm caudal from
686 bregma, 2.1 mm lateral from midline, 2.8-3.0 mm ventral from the cortical surface) of VGAT-cre mice
687 did not label cells inside the MGB, but instead induced Jaws expression in cre-expressing TRN cells
688 that project to the auditory thalamus. After the injection, we placed a 400 µm fibre optic cannula
689 immediately above audTRN. To maximize the light transmission to the transfected area of audTRN the
690 fibre optic cannula was implanted at a 22.5° angle (relative to the coronal axis). The anatomical
691 position was histologically confirmed after the end of the experiments. For optogenetic suppression,
692 we used a 120 mW/mm^2, 640 nm laser pulse (Toptica Photonics, Germany) of 150 ms length, which
693 started 25 ms before sound onset.

694 *Intersectional targeting and activation of S1-recipient neurons in the shell of the IC*
695 We induced expression of cre in neurons receiving projections from S1, by injecting 200 nL of AA1-
696 hSyn-cre into S1 (-0.8 and -1.0 mm caudal from bregma, 2.6 mm lateral from midline, and 0.9, 0.7, and
697 0.5 mm ventral from the cortical surface). This virus anterogradely and transsynaptically infected

698 neurons receiving projections from S1 and induced expression of cre in those neurons[37]. In order to
699 target expression of ChR2-YFP to IC neurons that receive input from S1, we also injected 200 nL of the
700 cre-dependent construct AAV5-DIO-ChR2-YFP into the lateral part of the IC. For optogenetic
701 activation, a 10 mW/mm^2, 465 nm LED pulse (Doric Lenses) was delivered through a 1 mm optic fiber
702 acutely positioned on the dura mater above the lateral part of the dorsal IC. Stimulation occurred
703 concurrently with, and for the duration of, sound stimulation (i.e. 50 ms).

704 *Suppressing excitatory neurons in S1 using pan-neuronal expression of Jaws*

705 To determine whether S1 is required for whisker-induced suppression of auditory thalamic responses,
706 we injected 380 nL of AAV8-hSyn-Jaws[75] into S1 (-0.8 and -1.0 mm caudal from bregma, 2.6 mm lateral
707 from midline, and 0.9, 0.7, and 0.5 mm ventral from the cortical surface) of mice genetically corrected
708 for age-related hearing loss (C57BL6/NTac.Cdh23[68]). For optogenetic suppression of S1 activity during
709 extracellular recordings in the auditory thalamus, a 5-7 mW/mm^2, 635 nm LED pulse (Doric Lenses)
710 was delivered through an acutely positioned 1 mm optic fibre optic placed on the dura mater above
711 S1. Light stimulation started 10 ms prior to the onset of sound stimulation and lasted 250 ms.

712 *Silencing excitatory cortical activity in VGAT-ChR2-YFP mice*

713 For optogenetic silencing of A1 and S1, we used a blue (465 nm) LED stimulus (duration 150 ms, onset
714 25 ms before auditory and/or somatosensory stimulation) delivered via a 200 µm optic fibre (Doric
715 Lenses) acutely implanted over the dura mater above A1 or the S1 barrel field, respectively. ChR2 was
716 targeted to inhibitory neurons using VGAT-ChR2-YFP mice. Light power was ~15 mW/mm^2.

717 ## Histology

718 For post-mortem verification of the electrophysiological recording sites, viral expression pattern, and
719 anatomical tracing, mice were overdosed with pentobarbital (100 mg/Kg body weight, i.p.;
720 pentobarbitone sodium; Merial Animal Health Ltd, Harlow, UK) and perfused transcardially, first with
721 0.1 M phosphate-buffered saline (PBS, pH 7.4) and then with fresh 4% paraformaldehyde (PFA,
722 weight/volume) in PBS. Mice used in anatomical experiments were euthanized and perfused >4 weeks
723 after the virus injections. Mice used for acute electrophysiology were perfused as soon as the
724 recordings were finished, while those used for chronic 2-photon imaging were perfused when all
725 imaging sessions were completed. Following perfusion, brains were kept in 4% PFA (weight/volume)
726 in PBS for ~24 hours. The relevant parts of the brains were then sectioned using a vibratome in the
727 coronal plane at a thickness of 50 or 100 µm. Sections were then mounted on glass slides and covered
728 in a mounting medium with DAPI (Vectashield, Vector Laboratories). Images were acquired with an
729 Olympus FV1000 confocal laser scanning biological microscope. Confocal images were captured using
730 similar parameters of laser power, gain, pinhole and wavelengths with two channels assigned as the

731 emission color; z-stacks were taken individually for each channel and then collapsed. Images were
732 processed offline using Imaris (Zurich, Switzerland) and ImageJ (NIH, MD, USA).

733

734 Data analysis and statistics

735 We clustered potential neuronal spikes using KiloSort[77] (https://github.com/cortex-lab/KiloSort).
736 Following this automatic clustering step, we manually inspected the clusters in Phy
737 (https://github.com/kwikteam/phy) and removed noise (movement artefacts, optogenetic light
738 artefacts etc). We assessed clusters according to suggested guidelines published by Stephen Lenzi and
739 Nick Steinmetz (https://phy-contrib.readthedocs.io/en/latest/template-gui/#user-guide). Each
740 cluster (following merging and noise removal) was assigned as either noise (clearly not neuronal spike
741 shape), multi-unit (neuronal and mostly consistent spike shape with no absolute refractory period), or
742 single unit (consistent spike shape with absolute refractory period). All analyses performed on the
743 electrophysiological data were run on a combination of small multi-unit clusters and single units (no
744 differences were found between them). Stimulus-evoked responses were measured as the mean firing
745 rate (spikes/second, sp/s) for the duration of the stimulus presentation. Baseline activity was
746 measured from the mean firing rate of the 90 ms preceding stimulus onset.

747 For 2-photon imaging of thalamocortical axons and boutons, we carried out standard
748 preprocessing (e.g. registration of image stacks, region of interest selection, trace extraction) of the
749 calcium data, as described in detail elsewhere[28,78]. Given the slower dynamics of GCaMP6m used to
750 monitor bouton activity from auditory thalamocortical axons, we measured the calcium transient
751 response to a 50 ms stimulus as the mean $\Delta F/F$ over the 16 frames following stimulus onset (i.e. for
752 ~550 ms). Baseline activity was measured as the mean $\Delta F/F$ over the 16 frames preceding stimulus
753 onset.

754 For estimation of somatosensory modulation of noise responses, we only included
755 units/boutons that showed a statistically significant response during sensory stimulation compared to
756 baseline (*t*-test, $p < 0.005$). For estimation of somatosensory modulation of tone responses, we only
757 included units/boutons that showed a statistically significant difference in response among the
758 frequency-level combinations tested (one-way ANOVA, $p < 0.005$).

759 The best frequency (BF) of tone-responsive neurons and boutons was defined as the sound
760 frequency associated with the largest response (i.e. firing rate or $\Delta F/F$, respectively) at the sound level
761 used. For summary statistics and display of summary frequency tuning curves across units/boutons,
762 we normalized the tuning curves of each unit/bouton. To do this, we first estimated the mean

763 frequency tuning curve across conditions (e.g. with and without whisker deflection and/or S1/A1
764 manipulations), and centered the frequency tuning curves for each condition on the BF estimated
765 from the mean frequency tuning curve. We then normalized the response to each tone frequency
766 presented - separately for each condition - by dividing by the response at the BF in the control
767 condition (i.e. tones presented alone). We then produced a summary frequency tuning curve by taking
768 the median of the normalized frequency tuning curves across units/boutons. Error bars for the
769 summary tuning curves were estimated from bootstrapped (10,000 iterations) 95% nonparametric
770 confidence intervals.

771 For group (i.e. across units or boutons) comparisons, we used non-parametric statistical tests
772 (i.e. Wilcoxon signed rank for paired samples and Mann–Whitney *U* test for independent samples).

773 Methods references

774 68. Mianné, J. *et al.* Correction of the auditory phenotype in C57BL/6N mice via CRISPR/Cas9-
775 mediated homology directed repair. *Genome Med.* **8**, 1–12 (2016).

776 69. Stiebler, I. & Ehret, G. Inferior colliculus of the house mouse. I. A quantitative study of tonotopic
777 organization, frequency representation, and tone-threshold distribution. *J. Comp. Neurol.* **238**,
778 65–76 (1985).

779 70. Portfors, C. V., Mayko, Z. M., Jonson, K., Cha, G. F. & Roberts, P. D. Spatial organization of
780 receptive fields in the auditory midbrain of awake mouse. *Neuroscience* **193**, 429–439 (2011).

781 71. Guo, W. *et al.* Robustness of cortical topography across fields, laminae, anesthetic states, and
782 neurophysiological signal types. *J. Neurosci.* **32**, 9159–9172 (2012).

783 72. Pologruto, T. A., Sabatini, B. L. & Svoboda, K. ScanImage: Flexible software for operating laser
784 scanning microscopes. *Biomed. Eng. Online* **2**, 1–9 (2003).

785 73. Klapoetke, N. C. *et al.* Independent optical excitation of distinct neural populations. *Nat.*
786 *Methods* **11**, 338–346 (2014).

787 74. Nagel, G. *et al.* Channelrhodopsin-2, a directly light-gated cation-selective membrane channel.
788 *Proc. Natl. Acad. Sci.* **100**, 13940–13945 (2003).

789 75. Chuong, A. S. *et al.* Noninvasive optical inhibition with a red-shifted microbial rhodopsin. *Nat.*
790 *Neurosci.* **17**, 1123–1129 (2014).

76. Tervo, D. G. R. *et al.* A designer AAV variant permits efficient retrograde access to projection neurons. *Neuron* **92**, 372–382 (2016).

77. Pachitariu, M., Steinmetz, N. A., Kadir, S., Carandini, M. & Harris, K. D. Kilosort: realtime spike-sorting for extracellular electrophysiology with hundreds of channels. http://www.biorxiv.org/content/10.1101/061481v1 (2016). doi:10.1101/061481

78. Barnstedt, O., Keating, P., Weissenberger, Y., King, A. J. & Dahmen, J. C. Functional microarchitecture of the mouse dorsal inferior colliculus revealed through in vivo two-photon calcium imaging. *J. Neurosci.* **35**, 10927–10939 (2015).